


RESEARCH

Open Access



Cathepsin B abundance, activity and microglial localisation in Alzheimer's disease-Down syndrome and early onset Alzheimer's disease; the role of elevated cystatin B

Yixing Wu¹, Paige Mumford¹, Suzanna Noy², Karen Cleverley², Alicja Mrzyglod¹, Dinghao Luo¹, Floris van Dalen^{3,4}, Martijn Verdoes^{3,4}, Elizabeth M. C. Fisher² and Frances K. Wiseman^{1*} 

Abstract

Cathepsin B is a cysteine protease that is implicated in multiple aspects of Alzheimer's disease pathogenesis. The endogenous inhibitor of this enzyme, cystatin B (*CSTB*) is encoded on chromosome 21. Thus, individuals who have Down syndrome, a genetic condition caused by having an additional copy of chromosome 21, have an extra copy of an endogenous inhibitor of the enzyme. Individuals who have Down syndrome are also at significantly increased risk of developing early-onset Alzheimer's disease (EOAD). The impact of the additional copy of *CSTB* on Alzheimer's disease development in people who have Down syndrome is not well understood. Here we compared the biology of cathepsin B and *CSTB* in individuals who had Down syndrome and Alzheimer's disease, with disomic individuals who had Alzheimer's disease or were ageing healthily. We find that the activity of cathepsin B enzyme is decreased in the brain of people who had Down syndrome and Alzheimer's disease compared with disomic individuals who had Alzheimer's disease. This change occurs independently of an alteration in the abundance of the mature enzyme or the number of cathepsin B⁺ cells. We find that the abundance of *CSTB* is significantly increased in the brains of individuals who have Down syndrome and Alzheimer's disease compared to disomic individuals both with and without Alzheimer's disease. In mouse and human cellular preclinical models of Down syndrome, three-copies of *CSTB* increases *CSTB* protein abundance but this is not sufficient to modulate cathepsin B activity. EOAD and Alzheimer's disease-Down syndrome share many overlapping mechanisms but differences in disease occur in individuals who have trisomy 21. Understanding this biology will ensure that people who have Down syndrome access the most appropriate Alzheimer's disease therapeutics and moreover will provide unique insight into disease pathogenesis more broadly.

Keywords Down syndrome, Alzheimer's disease, Cathepsin B, Cystatin B

*Correspondence:

Frances K. Wiseman

f.wiseman@ucl.ac.uk

Full list of author information is available at the end of the article



© The Author(s) 2023. **Open Access** This article is licensed under a Creative Commons Attribution 4.0 International License, which permits use, sharing, adaptation, distribution and reproduction in any medium or format, as long as you give appropriate credit to the original author(s) and the source, provide a link to the Creative Commons licence, and indicate if changes were made. The images or other third party material in this article are included in the article's Creative Commons licence, unless indicated otherwise in a credit line to the material. If material is not included in the article's Creative Commons licence and your intended use is not permitted by statutory regulation or exceeds the permitted use, you will need to obtain permission directly from the copyright holder. To view a copy of this licence, visit <http://creativecommons.org/licenses/by/4.0/>. The Creative Commons Public Domain Dedication waiver (<http://creativecommons.org/publicdomain/zero/1.0/>) applies to the data made available in this article, unless otherwise stated in a credit line to the data.

Introduction

People who have Down syndrome (DS) are at much greater risk of developing early-onset Alzheimer's disease (EOAD) than individuals from the general population, by the age of 55 around half of all people with DS will have been diagnosed with clinical dementia [1]. DS is caused by an extra copy of human chromosome 21 (Hsa21), which encodes ~221 protein-coding genes (Ensembl release 109—Feb 2023). The gene for Amyloid precursor protein (*APP*) is located on Hsa21, and duplication of this gene (*dupAPP*) is sufficient to cause EOAD in individuals who do not have DS [2] and is proposed to be both necessary and sufficient to trigger the early development of AD in individuals who have DS [3–5]. However, increasing evidence indicates that AD-relevant processes are modulated by Hsa21 trisomy, including the accumulation of amyloid- β [6–11] and the neuroinflammatory response to disease-associated pathology [12–16]. These differences are caused by the additional copy of gene(s) on Hsa21, resulting in elevated abundance of gene products that perturb molecular stoichiometry and lead to the changes in biology that occur in people who have DS. Understanding these differences in AD development in people who have DS is important for effective diagnosis and treatment, for this important group of individuals who are at greatly increased risk of dementia. Moreover, this research can provide unique mechanistic insight into the processes that contribute to disease pathogenesis.

Cathepsin B is a lysosomal cysteine protease, that has been implicated in important aspects of AD development, and a recent genome-wide association study has demonstrated an association of variation in the Cathepsin B gene (*CTSB*) with AD risk [17]. Raised levels of cathepsin B and increased activity are associated with AD and may be a potential therapeutic target, although aspects of the role of the enzyme in disease are debated [18]. These include the processing of APP via mediating its cleavage at the β -secretase site such that increased enzyme activity is proposed to raise the abundance of APP-C-terminal fragment β and amyloid- β [19]. This suggests that increased activity of the enzyme promotes AD development. However, research in other preclinical models has indicated that the enzyme has a role in the degradation of amyloid- β , and thus increased activity would lower amyloid- β and thus slow AD development [20]. In addition, cathepsin B has been proposed to have a key role in the neuroinflammatory responses to amyloid- β that mediates lysosomal damage signals and the induction of the inflammasome pathway in microglia [21, 22].

The abundance and activity of cathepsin B has been reported to be raised in DS fibroblasts but its activity in the brain is not well understood [23]. It is notable that

an endogenous inhibitor of cysteine cathepsins, cystatin B (*CSTB*) is encoded on Hsa21. This endogenous inhibitor does not target all lysosomal proteases, implicated in Alzheimer's disease, it does not impact the activity of Cathepsin D, which has recently been suggested to have a role in disease development via its function in amyloid- β and tau clearance [24]. How the additional copy of *CSTB* influences the changes to cathepsin B that occur during AD pathogenesis in people who have DS is not well understood. We hypothesize that trisomy of chromosome 21, will raise *CSTB* protein abundance in the brain and this will modulate the activity of cathepsin B in individuals who have DS when they develop AD compared to people with EOAD from the general population. Here we use a combination of studies in human post-mortem brain material and preclinical model systems to address this knowledge-gap.

Materials and methods

Summary tables of human post-mortem cases, fibroblasts and mouse numbers used

See Tables 1, 2, 3.

Animal welfare and husbandry

All experiments were undertaken in accordance with the Animals (Scientific Procedures) Act 1986 (United Kingdom), after local institutional ethical review by the Medical Research Council, University College London and results are reported in accordance with ARRIVE 2.0 guidelines.

Mice were housed in individually ventilated cages (Tecniplast) with grade 5, autoclaved dust-free wood bedding, paper bedding and a translucent red "mouse house". Free access to food and water was provided. The animal facility was maintained at a constant temperature of 19–23 °C with 55 ± 10% humidity in a 12-h light/dark cycle. Pups were weaned at 21 days and moved to standardised same-sex group housing with a maximum of 5 mice per cage.

The following mouse strains were used, here we show the abbreviated name and then the official name and unique Mouse Genome Informatics (MGI) identifier: *App*^{NL-F} (*App*^{tm2.1Tcs}, MGI:5637816), *Dp1Tyb* (*Dp(16Lipi-Zbtb21)1TybEmcf*, MGI:5703798) *Dp(10)2Yey* (*Dp(10Prmt2-Pdxk)2Yey*, MGI:4461400) and *Dp(17)3Yey* (*Dp(17Abcg1-Rrp1b)3Yey*, MGI:4461398). All mouse strains were maintained by backcrossing males and females to C57BL/6J mice (imported from the Jackson Laboratory) and for all strains used backcrossing had taken place for more than ten generations. For Fig. 6a–d *Dp(10)2Yey* mice were crossed with *App*^{NL-F/+} animals over two-generations to generate all required genotypes from the second generation (wild-type, *Dp(10)2Yey*), *App*^{NL-F/NL-F}, *Dp(10)2Yey;App*^{NL-F/NL-F}). All other

Table 1 Samples of human post-mortem temporal cortex (BA21) used for this research, including UK Brain Bank Identification Number (UK BBN ID), and anonymised demographics of the cases studied including Braak neurofibrillary tangle stage and *APOE* genotype, as reported by the SWDBB brain bank

UK BBN ID	Gender	Age at death (years)	PMI (hours)	<i>APOE</i>	Status	Braak
BBN_9061	F	54	24	3,3	AD	VI
BBN_9162	M	63	43	3,3	AD	VI
BBN_9212	F	65	22	3,3	AD	VI
BBN_9259	F	47	54	3,4	AD	VI
BBN_9265	F	60	5	2,3	AD	VI
BBN_9291	M	62	25	3,4	AD	VI
BBN_9315	F	67	24	4,4	AD	VI
BBN_9342	F	65	12	4,4	AD	VI
BBN_4202	M	64	67	4,4	AD	V
BBN_9406	M	61	33	2,3	AD	VI
BBN_8761	M	63	31	3,3	DS-AD	n/a
BBN_8867	M	62	24	3,4	DS-AD	VI
BBN_8869	M	62	51	3,3	DS-AD	V
BBN_8881	F	63	51	2,3	DS-AD	VI
BBN_8887	F	50	43	3,4	DS-AD	VI
BBN_8953	F	64	48	3,3	DS-AD	VI
BBN_8991	M	64	16	3,3	DS-AD	V
BBN_8994	F	59	24	3,3	DS-AD	VI
BBN_9097	F	67	17	3,4	DS-AD	VI
BBN_9184	F	48	79	2,4	DS-AD	IV
BBN_8696	M	63	40	3,3	Healthy-ageing	
BBN_8700	M	64	12	3,4	Healthy-ageing	
BBN_8702	M	58	20	2,3	Healthy-ageing	
BBN_8703	M	64	16	3,3	Healthy-ageing	
BBN_8835	F	73	59	3,3	Healthy-ageing	
BBN_8980	F	72	24	3,3	Healthy-ageing	
BBN_9389	F	68	39	2,3	Healthy-ageing	0
BBN_9399	F	73	50	3,4	Healthy-ageing	II
BBN_9422	F	74	40	3,3	Healthy-ageing	I
BBN_9432	F	74	28	N/A	Healthy-ageing	II

Table 2 Demographics for the human fibroblast lines used in this research, including Coriell Institute for Medical Research ID, and anonymised details of the donor

Coriell ID	Disomic/trisomy21	Age at donation (years)	Gender	Tissue source
GM05399	Disomic	1 year	M	Inguinal
GM05658	Disomic	1 year	M	Umbilical area
GM05758	Disomic	1 year	M	Inguinal
GM05565	Disomic	3 years	M	Inguinal
AG04823	Trisomy 21	5 years	M	Thorax
AG07438	Trisomy 21	9 months	M	Thorax
AG05397	Trisomy 21	1 year	M	Thorax
AG06922	Trisomy 21	2 years	M	Thorax

mouse cohorts (Fig. 6e–j) were generated by backcrossing to C57BL/6J mice. Animals were euthanized by exposure to rising carbon dioxide, followed by confirmation of death by dislocation of the neck in accordance with the Animals (Scientific Procedures) Act 1986 (United Kingdom).

Culture of human fibroblasts

Human fibroblasts from individuals who had DS and age and sex-matched disomic controls (kindly supplied by the Coriell Biorepository) were grown in Dulbecco's Modified Eagle Medium (DMEM) supplemented with 10% fetal bovine serum and 100 units/ml of penicillin–streptomycin (Thermo Fisher Scientific), at 37 °C with 5% CO₂. Cells were collected at 70% confluency by

Table 3 Summary information of the number and sex of individual mice used in this research

Cohort	WT (n)		Segmental duplication (n)		<i>App</i> ^{NL-F/NL-F} (n)		Segmental duplication; <i>App</i> ^{NL-F/NL-F} (n)	
	Male	Female	Male	Female	Male	Female	Male	Female
Dp(10)2Yey * <i>App</i> ^{NL-F/NL-F}	4	1	8	0	9	0	4	2
Dp(10)2Yey (ALLM)	3	5	4	2	N/A	N/A	N/A	N/A
Dp(10)2Yey (FMK)	3	3	8	5	N/A	N/A	N/A	N/A
Dp1Tyb	8	6	6	8	N/A	N/A	N/A	N/A
Dp(17)3Yey	4	4	4	4	N/A	N/A	N/A	N/A

trypsinisation (Gibco™ Trypsin-Ethylenediaminetetraacetic acid (EDTA) (0.25%), Thermo Fisher Scientific) and mechanical agitation, pelleted, and washed 3 times in phosphate buffered saline (PBS) prior to homogenization. Experiments were undertaken between passage number 7 and 17. All experiments were blinded for trisomy of Hsa21 or disomic status.

Cathepsin activity assays

Cathepsin B (CatB), and cathepsin D (CatD) endo-peptidase activity was determined using commercial assay kits (Cathepsin B: ab65300, Abcam; Cathepsin D: ab65302, Abcam). Samples were homogenized in lysis buffer as per the manufacturer's instructions, incubated on ice for 10–30 min, then centrifuged at 15,000×g for 5 min. Protein concentration of the resultant supernatant was determined by Bradford assay. For CatB assays, 40–100 µg homogenate was diluted in 50 µl CB lysis buffer from the Cathepsin B Activity Assay Kit (Fluorometric) (ab65300) and loaded into 96 well microplates (Greiner Bio-One flat black clear bottom). For CatD, 5–10 µg homogenate was loaded. 2 µl CatB inhibitors *N*-Acetyl-L-leucyl-L-leucyl-L-methioninal (ALLM) (Abcam, ab141446) or *Z*-Phe-Phe-FMK (Abcam, ab141386), and 3 µg Pepstatin A (Sigma) (an inhibitor of aspartyl proteases including CatD) were used for negative controls. The substrate (Ac-RR) labelled with amino-4-trifluoromethyl coumarin (AFC) was used for the CatB assay; and for CatD, GKPIFFRLK(Dnp)-D-R-NH₂ labelled with 7-methoxycoumarin-4-acetic acid (MCA) was used. Plates were incubated at 37 °C in the dark and fluorescence activity measured at Ex/Em λ 400/505 nm (CatB) and Ex/Em λ 328/460 nm (CatD) every 90 s over a period of 135 min on a Tecan fluorometric plate reader.

The rate of reaction, proportional to enzymatic activity, was calculated using the slope of the linear phase of the reaction for a minimum of 10 cycles and expressed as a % of the equivalent slope for the control samples. For fibroblast samples and samples of human temporal

cortex, an inhibited control was run for each individual sample used. For samples of mouse cortex, a representative inhibited control for each genotype was used. To control for non-specific activity, any activity detected in the appropriate inhibited control reaction was subtracted from the total activity observed in the uninhibited samples prior to analysis. Means of technical replicates were calculated for each individual sample, with biological replicate being used as the experimental unit. For CatB assays 4, 10 and 2–6 technical replicates were used for human post-mortem temporal cortex, fibroblasts and mouse cortex samples respectively. For CatD assays 2 technical replicates were run for each human post-mortem temporal cortex sample.

BMV109 staining and in-gel assay

For BMV109 staining of human fibroblasts, cells were incubated in Cellvis 6 Well glass bottom plates with high performance #1.5 cover glass (Fisher Scientific). For control wells to be pre-treated with cathepsin inhibitors, CA-074ME (Merck Millipore, 10µM) was added 30 min prior to the BMV109 preincubation. BMV109 (A kind gift from Dr Martijn Verdoes, RIMLS, Netherlands, 1 µM, 1:5,000) and LysoTracker™ Green DND-26 (Thermo Fisher Scientific, 50 nM, 1:20,000) were then added for 1 h and followed by 3 washes in PBS. Live cell imaging was then conducted by ZEISS LSM 980 confocal microscope (Carl Zeiss, Germany). A diode laser 488 was used for imaging LysoTracker Green (excitation 504 nm/emission 511 nm) and a diode laser 639 was used for imaging BMV109 (excitation 633 nm/emission 670 nm).

After confocal imaging, fluorescent sodium dodecyl sulphate–polyacrylamide gel electrophoresis (SDS-PAGE) was conducted by following Edgington-Mitchell et al. [25] with minor modifications. In brief, fibroblasts were lysed in CB Cell Lysis Buffer from Cathepsin B Activity Assay Kit (Abcam, ab65300). NuPAGE Lithium Dodecyl Sulphate (LDS) Sample Buffer (Thermo Fisher Scientific) and NuPAGE Sample Reducing Agent were

added to the samples, which were then heated for 5 min at 95 °C. SDS-PAGE was conducted by running samples on NuPAGE Novex 4–12% Bis-Tris Protein Gels in ((3-(N-morpholino)propanesulfonic acid (MOPs) or its structural analogue 2-(N-morpholino)ethanesulfonic acid (MES) SDS running buffer (both Thermo Fisher Scientific) at 120 V for 1.5 h. After SDS-PAGE, the gel was taken to be imaged by the 700 Channel Laser Source (excitation 685 nm /emission 720 nm) of Odyssey DLx Fluorescence Imaging System (LI-COR Biosciences). After imaging, the gel was transferred directly into the Bio-Safe™ Coomassie Stain (BIO-RAD, #1,610,786) and incubated overnight at 4 °C with agitation. The gel was then taken to be imaged by Odyssey DLx Fluorescence Imaging System (LI-COR Biosciences).

Western blotting

Human fibroblasts were lysed in M-PER Mammalian Protein Extraction Reagent (Thermo Fisher Scientific) supplemented with cOmplete protease and PhosSTOP phosphatase inhibitors (Roche). Human temporal cortex samples were lysed in CB Cell Lysis Buffer from the Cathepsin B Activity Assay Kit (Abcam, ab65300). Mouse cortex samples were lysed in RIPA buffer (150 mM sodium chloride, 50 mM Tris, 1% NP-40, 0.5% sodium deoxycholate, 0.1% SDS) plus complete protease inhibitors (Calbiochem) by mechanical disruption.

Samples were denatured in NuPAGE LDS Sample Buffer (Thermo Fisher Scientific) and NuPAGE Sample Reducing Agent in a 95 °C heat block for 5 min. Samples were then loaded into NuPAGE Novex 4–12% Bis-Tris Protein Gels in MOPs or MES SDS running buffer (both Thermo Fisher Scientific) and SDS-PAGE was conducted by the application of 200 V for 50 min or 120 V for 1.5 h. The proteins in the gel were transferred to a polyvinylidene difluoride (PVDF) membrane by Trans-Blot® Turbo™ Transfer System (Bio-Rad Laboratories) at 25 V, 2.5 A, for 7 min. The membranes were blocked with Intercept (PBS) Blocking Buffer (LI-COR Biosciences) for 1 h at room temperature. The membranes were then incubated in primary antibodies in Intercept (PBS) Blocking Buffer (LI-COR Biosciences) overnight with agitation at 4 °C. The membranes were washed three times in PBS with 1% Tween20 (PBST) for 10 min before application of IRDye 680RD or 800CW secondary antibodies (LI-COR Biosciences) for 1 h at room temperature: both at 1:10,000 dilutions in Intercept (PBS) Blocking Buffer (LI-COR Biosciences). After antibody probing, membranes were subjected to another three 10-min washes with PBST, and images were then taken by Odyssey DLx Fluorescence Imaging System (LI-COR Biosciences). The density of protein bands was analysed with ImageJ. β -actin or GAPDH was used for the normalisation of

CSTB and CatB protein levels. Relative intensities were calculated by dividing the lane density by the healthy ageing or WT within gel average density.

The primary antibodies are rabbit polyclonal anti-cystatin-B (Abcam, ab236646, 1:2,000), anti-cathepsin B (Abcam, ab92955, 1:1,000 and Merck, Ab-3 1:100) and anti- β -actin mouse monoclonal antibody (Sigma-Aldrich, #A5441, 1:5,000). The secondary antibodies were IRDye 800CW Goat anti-Rabbit IgG (H+L) (1:10,000) and IRDye 680RD Goat anti-Mouse IgG (H+L) (1:10,000) (LI-COR Biosciences).

Immunostaining (fibroblasts)

Human fibroblasts were cultured on coverslips in 12 or 24-well plates. Cells were first washed with PBS, then fixed with 4% paraformaldehyde (PFA) for 10 min. After three PBS washes, cells were permeabilised with PBS with 0.1% Triton X-100 (Sigma-Aldrich). Cells were then blocked for 1 h at room temperature in blocking solution containing 5% goat serum, Tween-20 (Bio-Rad), and Glycine (Sigma-Aldrich) to prevent non-specific antibody binding. The cells were then stained with primary antibodies overnight at 4 °C in a humidified chamber. After primary antibody incubation, cells were washed with PBS with 0.1% Triton X-100, three times prior to one-hour secondary antibody incubation at room temperature. After secondary antibody incubation, cells were subjected to another three washes with PBST and mounted with Invitrogen ProLong Gold Antifade Mountant with 4',6-Diamidino-2-Phenylindole, Dihydrochloride (DAPI) (Thermo Fisher Scientific). Images were then taken by ZEISS LSM 980 confocal microscope (Carl Zeiss, Germany).

The primary antibodies are rabbit polyclonal anti-cystatin-B (Abcam, ab236646, 1:200), anti-cathepsin B (Abcam, ab92955, 1:500) and mouse anti-LAMP1 (Cell Signalling, #15,665, 1:100). The secondary antibodies were Goat anti-Rabbit IgG (H+L) Highly Cross-Adsorbed Secondary Antibody, Alexa Fluor™ Plus 488 (Thermo Fisher Scientific, A32731, 1:700) and goat-anti-rabbit-IgG-H-L-highly-cross-adsorbed-secondary-antibody-polyclonal (Thermo Fisher Scientific, A11004, 1:700).

Immunostaining (human post-mortem brain material)

To deparaffinise the samples, slides were first treated with xylene for three 5-min intervals, followed by 20–30 dips in 100%, 90% and 70% ethanol, and then 20–30 dips in water. Antigen retrieval was then carried out by placing the slides in 10 mM citrate buffer, pH 6, and heated in a microwave for 5 min at high power. After cooling for 3 min, the slides were heated for 2 min at high power, followed by another 3 min at high power after cooling.

The slides were then washed in water for 10 min with agitation, followed by 3 washes in PBS with 0.2% triton X-100, for 10 min each with agitation. The samples were then preincubated with blocking buffer (PBS, 0.2% triton X-100, and 5% Donkey serum) for 1 h at room temperature in a humid chamber. Primary antibodies (goat anti-IBA1 (Abcam ab5076, 1:100) and rabbit anti-Cathepsin B (Calbiochem, #PC41, 1:100)) were added to the blocking solution and incubated overnight at 4 °C in the humid chamber. After overnight incubation, the samples were washed in PBS and 0.2% triton for 3 times, 10 min each, and then secondary antibodies (Alexa Fluor 647 donkey anti-Rabbit (Invitrogen, #A31573, 1:500) and donkey anti-Goat IgG H&L Alexa Fluor 488 (Abcam, ab150129, 1:500)) diluted in blocking buffer were added to the samples and incubated for 1 h at room temperature in the humid chamber. The samples were then washed in PBS and 0.2% triton for 3 times, 10 min each, and DAPI was added for nuclear counterstain. The samples were incubated in DAPI solution for 5 min, then washed in PBS. Slides were incubated with TrueBlack Plus Lipofuscin Autofluorescence Quencher (Cambridge Bioscience, BT23014, 1:40 dilution in PBS) for 20 min, followed by washing in PBS. Then samples were mounted in Pro-Long Antifade Mountant (Thermo Fisher Scientific) and imaged by ZEISS LSM 980 confocal microscope (Carl Zeiss, Germany).

For each case two slides were stained and analysed. For each slide, 10 fields were chosen randomly and imaged using a 20× objective lens with a 426.67 μm × 426.67 μm total size per image. The images were exported as TIF files. To count the cells, the Cell Counter plugin (FIJI for ImageJ) was used. Any cell with red or green pixels within a proximity of 20 μm to a DAPI stained nucleus was identified as a cathepsin B or IBA1 positive cell.

Nuclear sub-fractionation

Nuclear and cytoplasmic sub-fractionations of human fibroblasts were carried out by using NE-PER™ Nuclear and Cytoplasmic Extraction Reagents (CER) (Thermo Fisher Scientific) as per the manufacturer's instructions. In brief, human fibroblasts were resuspended by trypsinisation (Gibco™ Trypsin–EDTA (0.25%) (Thermo Fisher Scientific)) and then centrifuged at 500×g for 5 min. The cell pellet containing approximately 1×10^6 cells was then washed with PBS prior to transferring to a 1.5 mL Eppendorf tube. Cells were then centrifuged at 500×g for 2–3 min. The supernatant was removed, and the cell pellet resuspended in ice-cold CER I. The tube was then vortexed on the highest speed for 15 s and the resuspended cells incubated on ice for 10 min. Ice-cold CER II buffer was added and the tube vortexed again for 5 s. The tube was incubated on ice for 1 min and then vortexed again

for 5 s. The cell lysate was then centrifuged for 5 min at maximum speed (~16,000×g) at 4 °C. The supernatant, which contains the cytoplasmic fraction was transferred to a new pre-chilled tube and stored at –80 °C for further use. The remaining pellet fraction containing the nuclei was resuspended in ice-cold NER and vortexed again. The sample was placed on ice and the 15-s vortexing step was repeated every 10 min for 40 min in total. The tube was then centrifuged at maximum speed (~16,000×g) for 10 min at 4 °C. The supernatant that contained the nuclear extract fraction was transferred to a new pre-chilled tube.

Cytoplasmic and nuclear fractions were then subjected to western blotting and labelled with rabbit monoclonal anti-GAPDH (Sigma, G9545, 1:5,000) antibody and rabbit polyclonal anti-LSD1 antibody (Abcam, ab129195, 1:2,500).

Experimental design and statistical analysis

Individual post-mortem brain donor, independent cell-line or individual animals were used as the unit of replication. Unique identification numbers were assigned to all samples to ensure the study remained blind and randomised during data acquisition and analysis. Statistical analysis was carried out using SPSS Statistics 22 (IBM) for ANOVA and Prism8 (GraphPad) for simple linear regression and Mann–Whitney U tests. When ANOVA was used for analysis, for studies of human post-mortem brain, gender and case type (healthy ageing, EOAD or AD-DS) were used as variables and age at death and post-mortem interval (PMI) as covariates; for mouse tissue studies genotype and sex of animal were used as variables. For fibroblast experiments, as the group sizes were small the non-parametric Mann–Whitney U test was used for analysis with disomy/trisomy of Hsa21 status as the variable. The mean of technical replicates was used for biochemical datasets and cellular immunofluorescence data. Repeated measures ANOVA was used for immunofluorescence data from cases of human post-mortem brain, slide 1 and slide 2 treated as repeated measures.

To determine the colocalisation between two proteins (i.e., fluorescence channels) in an image [26], Pearson's coefficient of colocalisation (R) was used, which quantifies the covariance/linear relationship between the intensities of the two channels, in this case including the fluorescence signal from the BMV-109 probe. To determine the intensity proportion of one channel within another channel, the Manders' coefficient was used. It quantifies the intensity proportion of channel x that overlaps with channel y.

Graphs were plotted using Prism8 (GraphPad), data are presented as mean ± Standard Error of the Mean

(SEM), p -values less than 0.05 are considered to be statistically significant.

Results

Case demographics

In this study we compared cases of EOAD (without known causal mutations in *APP*, *PSEN1* or *PSEN2*), Alzheimer's disease in individuals who had DS (AD-DS), and healthy ageing disomic individuals. All cases were sourced from the South West Dementia Brain Bank (SWDBB), University of Bristol, UK and were matched as far as possible for demographics (Tables 1 and 4). The gender of individuals did not differ between case types (four male and six female cases per group). The cases of healthy ageing used in this study were significantly older than EOAD and AD-DS but no significant differences in age occurred between EOAD and AD-DS groups (ANOVA $F(2,27)=5.651$, $p=0.009$; pairwise comparison with Bonferroni correction healthy ageing compared with EOAD $p=0.028$ with AD-DS $p=0.017$). No significant difference in PMI was found between case type (ANOVA $F(2,27)=0.487$, $p=0.620$). No significant difference was observed in the number of cases that had a *APOE* 2/3, 2/4 alleles compared with 3/3 alleles or with 3/4, 4/4 alleles ($\chi^2(2, 29)=1.945$, $p=0.745$). However, *APOE* 4/4 homozygotes were only observed in the EOAD group, likely contributing to the early development of disease in these individuals. The majority of cases of EOAD and AD-DS were Braak neurofibrillary tangle stage VI [27], one case of EOAD and two cases of AD-DS were Braak stage V, one case of AD-DS was Braak stage IV and insufficient material was available to stage one AD-DS case. In this study all samples were of temporal cortex Brodmann Area 21.

Three copies of *CSTB* increase the abundance of *CSTB* protein in the brains of individuals with AD-DS compared with those who have EOAD

Hsa21 encodes the endogenous inhibitor of cysteine cathepsins, cystatin B gene (*CSTB*). To determine if trisomy 21 results in an increase in *CSTB* protein in the brains of people who have AD-DS, we compared the abundance of the protein between these individuals and individuals from the general population with EOAD or who were ageing healthily, by western blot. The abundance of *CSTB* was significantly higher in cases of people who had AD-DS than in those from the general population who had EOAD or those that did not have dementia (healthy ageing) (Fig. 1a–d). The age and sex of the individual and the post-mortem interval did not significantly affect *CSTB* abundance. Thus, three-copies of *CSTB* resulting from trisomy of Hsa21, is associated with increased *CSTB* protein in the brains of people who have AD-DS compared to disomic individuals who have EOAD or are ageing healthily.

Down syndrome does not alter the abundance of mature cathepsin B in the brain but cathepsin B activity is lower in AD-DS than EOAD

In the same post-mortem samples, we quantified the abundance of mature cathepsin B protein (~28 kDa), by western blot using two independent antibodies (Ab-3 and ab92955). We found no significant change in the abundance of mature cathepsin B protein between the subgroups of cases with either antibody (Fig. 1a, b, e, f). Post-mortem interval, age and gender did not significantly affect the abundance of mature cathepsin B.

As *CSTB* protein abundance was elevated in individuals who had AD-DS we went on to investigate if cathepsin B endo-peptidase activity was impacted by the increase in the endogenous inhibitor. Using the same samples,

Table 4 Down syndrome Alzheimer's disease (AD-DS) and matched disomic Alzheimer's disease (EOAD) and healthy ageing case details. Summary of case demographics information of human post-mortem cases from matched disomic healthy ageing, EOAD and AD-DS cases, including age at death, post-mortem-interval, *APOE* genotype and Braak Tangle Stage

	Healthy ageing	EOAD	AD-DS
Gender	4 Male, 6 Female	4 Male, 6 Female	4 Male, 6 Female
Age at death (years)	68.3 ± 5.72	60.8 ± 6.03	60.2 ± 6.25
Post-mortem interval (h)	32.86 ± 15.27	30.73 ± 18.88	38.40 ± 19.74
<i>APOE</i> genotype (number of individuals)	2/3, 2/4 (2), 3/3 (5), 3/4, 4/4 (2), unknown (1)	2/3, 2/4 (2), 3/3 (3), 3/4, 4/4 (5)	2/3, 2/4 (2), 3/3 (5), 3/4, 4/4 (3)
Braak Tangle Stage (Number of individuals)	Not staged (6) 0 (1), I (1), II (2)	V (1) VI (9)	Not staged (1) IV (1) V (2) VI (6)

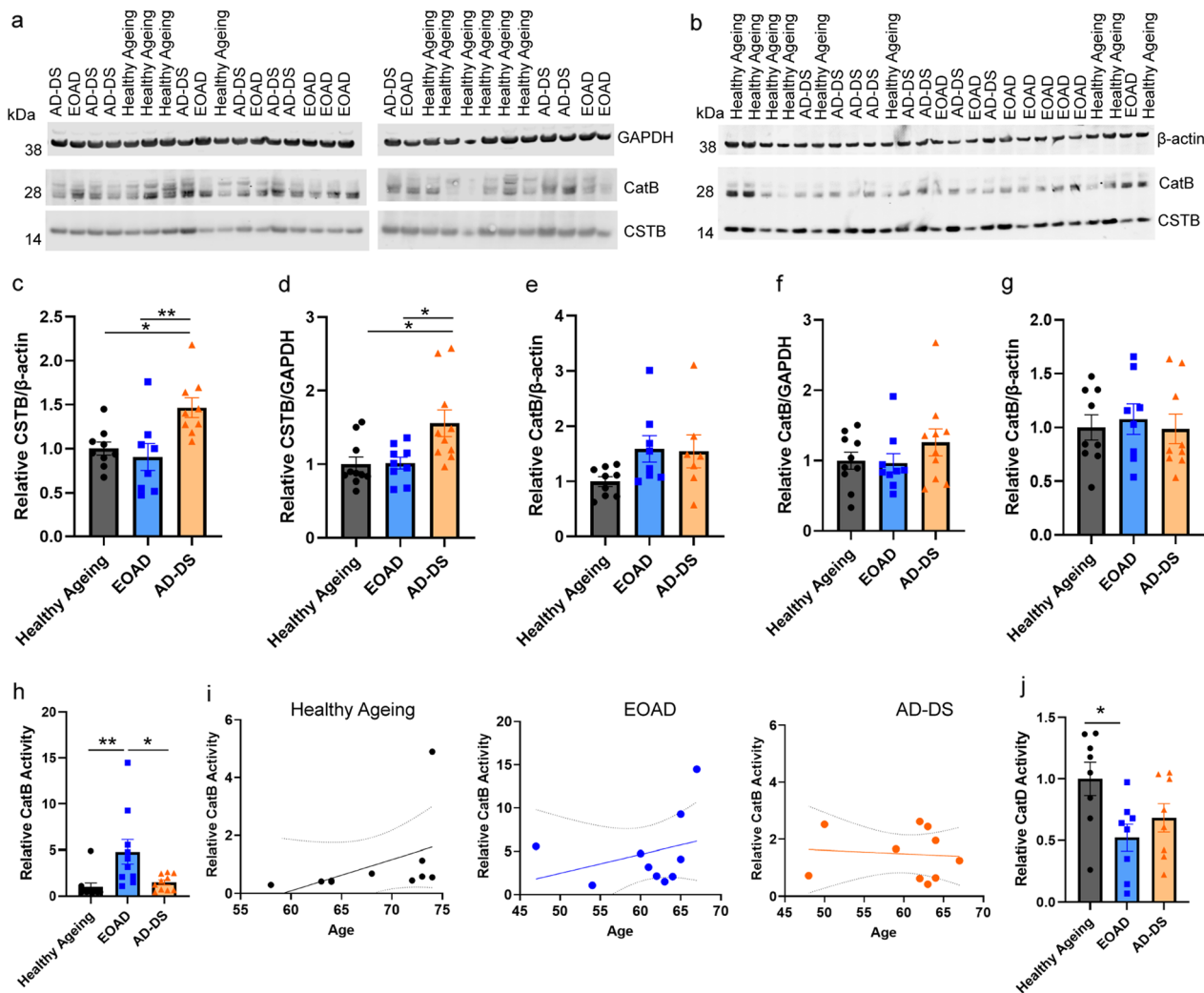


Fig. 1 Cystatin B (CSTB) abundance is increased and cathepsin B activity is reduced in the brains of individuals with AD-DS, independently of changed cathepsin B protein level or cathepsin D activity. Cystatin B (CSTB) (a–d) and cathepsin B (a, e, f Ab-3 or b, g ab92955), protein abundance measured by western blot in human temporal cortex from people who had AD-DS, EOAD and healthy ageing. c, d Type of case altered the abundance of CSTB protein (ANOVA β-actin $F(2,18)=9.087, p=0.002$; GAPDH $F(2,21)=7.500, p=0.003$). CSTB abundance was higher in individuals who had AD-DS than those with EOAD (pairwise comparisons with Bonferroni correction β-actin $p=0.008$, GAPDH $p=0.020$) and healthy controls from the general population (pairwise comparisons with Bonferroni correction, β-actin $p=0.024$; GAPDH $p=0.013$), with no difference in abundance between individuals with EOAD and control individuals (pairwise comparisons β-actin and GAPDH $p=1.000$). e–g The abundance of mature cathepsin B protein, e, f Ab-3 or g ab92955, was not altered by the type of case (Ab-3 ANOVA β-actin $F(2,16)=3.051, p=0.075$; GAPDH $F(2,21)=2.141, p=0.143$) (ab92955 ANOVA $F(2,18)=0.970, p=0.398$). h Type of case affected cathepsin B activity (ANOVA $F(2,22)=9.027, p<0.001$); activity was significantly higher in individuals who had EOAD than in controls (pairwise comparisons with Bonferroni correction $p=0.004$), but lower in individuals with AD-DS than those with EOAD (pairwise comparisons with Bonferroni correction, $p=0.012$), with no difference between individuals with AD-DS and control individuals (pairwise comparisons $p=1.000$). (i) Within case types, no significant correlations between age (in years) at time of death were observed (simple linear regression, Healthy ageing $r^2=0.1962, p=0.199$, EOAD $r^2=0.0989, p=0.376$ and AD-DS $r^2=0.0079, p=0.807$). j Type of case significantly affected cathepsin D activity (ANOVA $F(2,16)=6.360, p=0.009$); activity was significantly lower in individuals who had EOAD than in healthy controls (pairwise comparisons with Bonferroni correction $p=0.022$), no significant difference in activity was observed between AD-DS and healthy ageing controls (pairwise comparisons with Bonferroni correction, $p=0.180$), with no difference between individuals with AD-DS and those with EOAD (pairwise comparisons $p=1.000$). Individual data points are technical means for independent biological samples, error bars SEM. * $p<0.05$ and ** $p<0.01$

we measured cathepsin B activity by biochemical assay; quantifying the rate of cleavage of Ac-RR labelled with amino-4-trifluoromethyl coumarin (AFC). To control

for the non-specific activity, we measured the rate of cleavage in each sample inhibited by FMK(z-FA-FMK), a cysteine protease inhibitor. This non-specific activity

was then subtracted from the total activity to identify the proportion of the activity specific to cathepsin B. Using this method, we observed that cathepsin B activity is elevated in the temporal cortex of people who had EOAD compared with healthy controls, but that no difference in cathepsin B activity was observed in individuals who have AD-DS compared to healthy ageing controls (Fig. 1h). Moreover, significantly less cathepsin B activity was measured in the temporal cortex of individuals who have AD-DS compared with individuals from the general population who had EOAD. A previous report observed that the age of an individual significantly affects cathepsin B activity [28]. Thus, we investigated if a relationship between age at death and enzyme activity occurred in our samples by simple linear regression within case-type. We found no significant correlation between age of an individual at death and enzyme activity in healthy controls, or individuals with EOAD or AD-DS (Fig. 1i).

To understand if the change in cathepsin B activity was specific, we assayed the activity of another major lysosomal protease (cathepsin D); the activity of which is not regulated by *CSTB* [18]. We measured cathepsin D activity by the rate of cleavage of GKPIILFFRLK(Dnp)-D-R-NH₂ labelled with MCA. To control for non-specific activity, we measured the rate of cleavage in each sample inhibited by Pepstatin A, a cathepsin D inhibitor. This non-specific activity was then subtracted from the total activity to identify the proportion of the cleavage specific to cathepsin D. We found that cathepsin D activity was significantly decreased in the temporal cortex of individuals who had EOAD compared to the activity observed in healthy ageing control individuals (Fig. 1j). A similar pattern of decreased cathepsin D activity was also observed in samples of temporal cortex from individuals who have AD-DS, but this did not reach statistical significance. No difference in activity was detected between individuals who had AD-DS and those who had EOAD. These data are consistent with a decrease in cathepsin D activity reported in DS patient fibroblasts [23].

These data indicate that having three copies of *CSTB*, raises the abundance of *CSTB* protein in the brains of individuals who have AD-DS. This may cause the specific decrease in cathepsin B activity observed in the brains of people who have AD-DS compared to the raised activity of the enzyme which occurs in people who have EOAD.

Differences in cathepsin activity between EOAD and AD-DS are not the result of differences in Braak neurofibrillary tangle stage

In the case series studied, two cases of AD-DS were Braak neurofibrillary tangle stage V, one case was Braak stage IV and one case has not been staged. In comparison, only one EOAD case was Braak V and the other EOAD cases

were Braak VI. To determine if differences in Braak tangle stage contributed to the difference in cathepsin activity between EOAD and AD-DS, we repeated our analysis comparing AD-DS (Braak VI, 6 cases) with EOAD (Braak VI, 9 cases) and healthy ageing (Braak 0-II, 10 cases). In this sub-analysis, cathepsin B activity was significantly different between case types (ANOVA $F(2,17)=6.792$, $p=0.007$), with activity being significantly higher in EOAD compared with healthy ageing (pairwise comparison with Bonferroni $p=0.008$) but not different between AD-DS and healthy ageing (pairwise comparison with Bonferroni $p=1.000$) (Additional file 1: Supplementary Fig. 1a). In this sub-set of the cases, cathepsin D activity significantly differed between case types (ANOVA $F(2,14)=7.188$, $p=0.007$), with activity being significantly lower in EOAD compared with healthy ageing (pairwise comparison with Bonferroni $p=0.028$), activity did not significantly differ in AD-DS compared with healthy ageing (pairwise comparison with Bonferroni $p=0.070$) and no difference in the activity was observed between AD-DS and EOAD (pairwise comparison with Bonferroni $p=1.000$) (Additional file 1: Supplementary Fig. 1b). Thus, the difference in cathepsin B activity we observed in the cases of AD-DS compared with EOAD is likely to be caused by a specific effect of three copies of *Hsa21* on enzyme function and not the result of differences in tau pathology in the cases.

The number of IBA⁺ microglia and cathepsin B⁺ cells are upregulated in individuals who had EOAD and those who have AD-DS

Recent data has shown that the biology of microglia differs in people who have DS both prior to and after the development of AD pathology [13, 14, 29]. As cathepsin B is upregulated in microglia during the development of AD, we investigated if the changes in cathepsin B activity we observe in individuals who have DS, are related to changes in microglia. To identify microglia, we used an antibody against Ionized calcium binding adaptor molecule 1 (IBA1), which is expressed by microglia and macrophages. We quantified the number of IBA⁺ microglia, the number of cathepsin B⁺ cells, the proportion of cathepsin B colocalised with IBA⁺ microglia and the relative proportion of IBA⁺ microglia that contain cathepsin B, in samples of temporal cortex from people who had EOAD, AD-DS or healthy ageing (Fig. 2). We find that the number of IBA⁺ cells is significantly increased in people who have EOAD and those with AD-DS compared with those undergoing healthy ageing (Fig. 2d). However, no difference in the total number of IBA⁺ cells was observed when people who had AD-DS and those who had EOAD were compared. Similarly, the number of cathepsin B⁺ cells is significantly increased in people who had EOAD

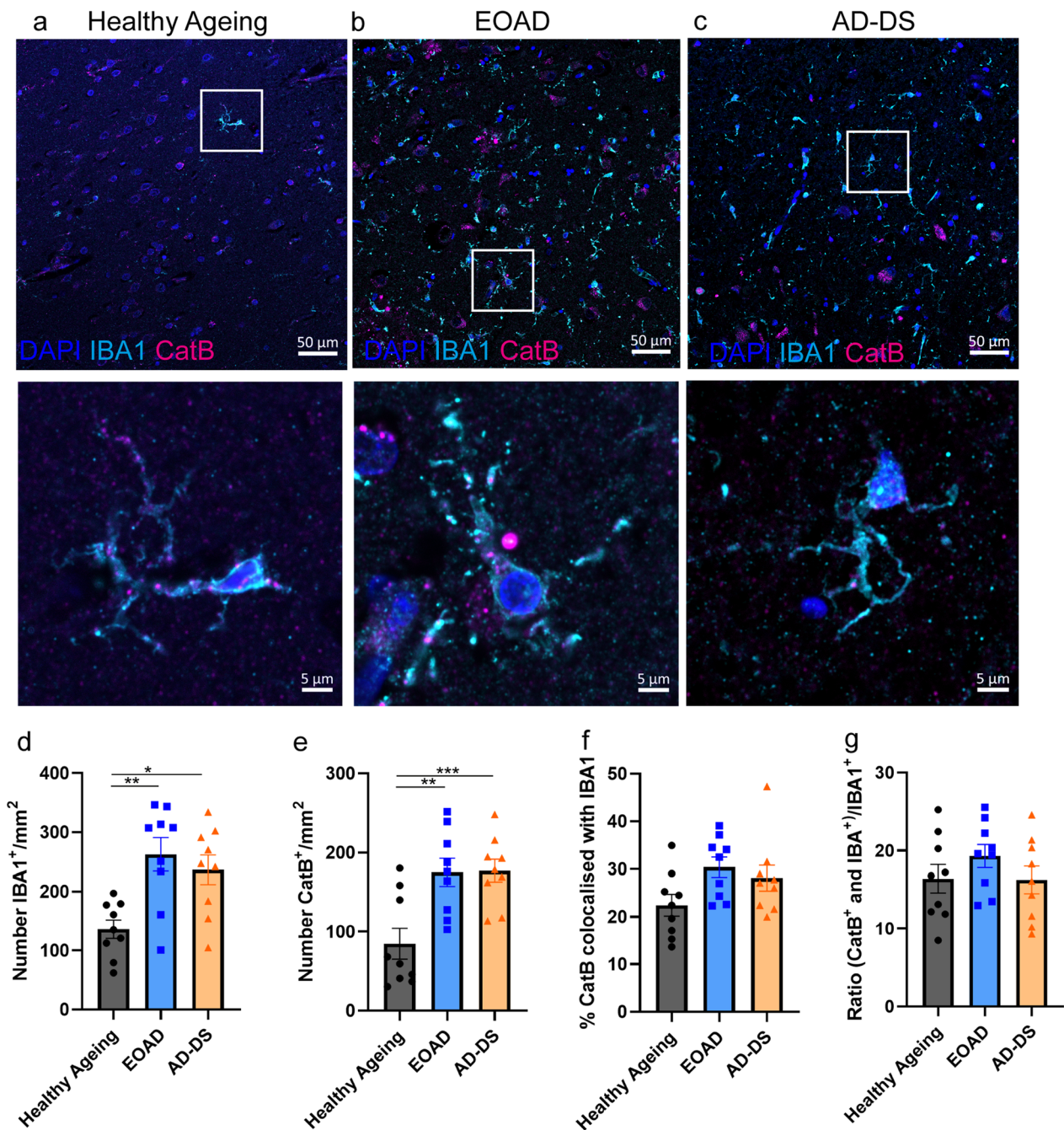


Fig. 2 The number of IBA1⁺ microglia and cathepsin B⁺ cells is increased in EOAD and AD-DS compared with healthy ageing but no change in the proportion of cathepsin B⁺ microglia occurs. **a–c** Representative images of IBA1 (cyan), cathepsin B (magenta) and DAPI-nucleus (blue) stained cells, and colocalised IBA1 and cathepsin B staining in human temporal cortex from individuals with **a** healthy ageing, **b** EOAD or **c** AD-DS. **d** The number of IBA1⁺ microglia/mm² was significantly altered by the type of case (ANOVA F(2,19) = 6.527, *p* = 0.007); significantly more cells were observed in both cases of EOAD and AD-DS compared with healthy ageing (pairwise comparisons with Bonferroni correction EOAD *p* = 0.005, AD-DS *p* = 0.028) but no difference was observed between EOAD and AD-DS. **e** The number of cathepsin B⁺ cells/mm² was significantly altered by the type of case (ANOVA F(2,19) = 13.379, *p* < 0.001); significantly more cells were observed in both cases of EOAD and AD-DS compared with healthy ageing controls (pairwise comparisons with Bonferroni correction EOAD *p* = 0.002, AD-DS *p* < 0.001) but no difference was observed between EOAD and AD-DS. **f** The proportion of total cathepsin B staining that colocalised with IBA1⁺ microglia was not altered by case type (ANOVA F(2,19) = 3.446, *p* = 0.053). **g** The proportion of IBA1 microglia that were also positive for cathepsin B was not altered by case type (ANOVA F(2,19) = 1.493, *p* = 0.250). **p* < 0.05, ***p* < 0.01 and ****p* < 0.001

or AD-DS compared with those who were undergoing healthy ageing but no difference in the number of cathepsin B positive cells occurred between individuals who had AD-DS and EOAD (Fig. 2e).

Case type did not alter the proportion of total cathepsin B staining that colocalised with IBA1⁺ (Fig. 2f). Notably, the majority (~70%) of cathepsin B staining did not colocalise with IBA1, indicating that the bulk of activity in the brain likely occurs in other cell-types (including microglia that do not express IBA1) or extracellularly. Moreover, case type did not affect the proportion of IBA⁺ microglia cells that were positive for cathepsin B (Fig. 2g). These data indicate that the differences observed in the activity of cathepsin B enzyme in people who have AD-DS are not related to the number of cells expressing the enzyme, consistent with our western blotting data. Nor does the distribution of the enzyme in microglia differ between individuals who have EOAD and AD-DS. Thus, the specific reduction in activity in individuals who have AD-DS compared to those who have EOAD, likely occurs by an alternative mechanism and is not caused by a change in the distribution of the enzyme to microglia cells.

Trisomy Hsa21-associated cathepsin B deficits are not modelled in human fibroblasts, despite the raised abundance and unchanged subcellular distribution of CSTB

To test the hypothesis that raised CSTB, caused by an additional copy of Hsa21 causes the changes to cathepsin B activity in the brains of individuals who have AD-DS, we measured CSTB and cathepsin B protein abundance, and cathepsin B activity in fibroblasts isolated from infants and children who have DS (trisomy 21) and matched disomic individuals (Table 2). We first determined if three copies of *CSTB* lead to the raised abundance of CSTB protein, by western blot of total cellular proteins (Fig. 3a, b). Consistent with our results from human post-mortem brain material, an additional copy of Hsa21 significantly increased CSTB protein in fibroblasts, isolated from individuals who have DS.

Total cellular cathepsin B activity was measured using a biochemical fluorescence cleavage assay and no significant difference was observed between disomic and trisomy 21 cells (Fig. 3c). To investigate this further we assayed the activity of cathepsin B in disomic compared to trisomy 21 cells, using the activity-based probe BMV109 [30] (Fig. 3d). BMV109 is a small molecule probe, which carries an electrophilic moiety that covalently binds the cysteine cathepsin enzyme active site. This reaction releases the probes quenching group, resulting in the emission of fluorescence. The probe-binding is covalent and irreversible, and the resultant

fluorescence can be measured in both intact cells and isolated proteins subjected to SDS-PAGE separation. No significant difference in either total (Fig. 3d) or lysosomal (Fig. 3e) cathepsin B activity was observed between trisomy 21 and disomic fibroblasts using this method. This suggests that in fibroblast cells, three copies of Hsa21 raises CSTB protein levels, but this is not sufficient to modulate cathepsin B activity.

CSTB has been reported to be localised to the cytosol, nucleus and lysosome [31, 32]; the pattern of subcellular localisation of the protein is critical to its regulation of cathepsin activity. Thus, we determined if three copies of Hsa21 altered the subcellular distribution of CSTB and hence its impact on cathepsin activity, using biochemical subcellular fractionation and western blotting. We found no difference in the relative abundance of CSTB in the nucleus and cytoplasm in trisomy 21 compared to disomic fibroblasts and confirmed that total abundance of the protein was raised by three copies of Hsa21 (Fig. 4a–c). We determined if trisomy 21 altered the relative amount of CSTB that colocalised with LAMP1 (a lysosomal marker) in fibroblasts (Fig. 4d–e), as cathepsin activity in lysosomes is likely to have a particularly important role in APP processing and amyloid- β catabolism. We found no difference in colocalisation of CSTB and LAMP1 between trisomy 21 and disomic cells.

To determine if raised CSTB led to a compensatory alteration in cathepsin B protein abundance or processing; we quantified the amount of pro- and mature cathepsin B, generated by cleavage of the pro-form in trisomy 21 and disomic fibroblasts by western blotting. No differences in the relative abundance of pro- or mature cathepsin B were detected (Fig. 5a–c). Changes in the processing of cathepsin B were also not detected as measured by the ratio of the mature to pro-forms of the protein (Fig. 5d). We also determined if trisomy 21 altered the colocalization of cathepsin B with LAMP1 in fibroblasts (Fig. 5e, f). We found no difference in the proportion of cathepsin B colocalised with LAMP1 between disomic and trisomy 21 cells (Fig. 5e, f). Thus, the changes in cathepsin activity in the brains of people who have AD-DS are not modelled in a fibroblast model of trisomy of Hsa21 and may be specific to the central nervous system.

Three copies of *Cstb* increase CSTB abundance in the cortex of mouse models of AD-DS but do not alter Cathepsin B activity

To determine if an additional copy of *Cstb* is sufficient to raise CSTB protein abundance or alter cathepsin B enzyme activity in the adult brain of a mouse model of DS, we measured CSTB protein level and cathepsin activity in the Dp(10)2Yey mouse model, which has an additional copy of 38 genes, carried on an internal duplication

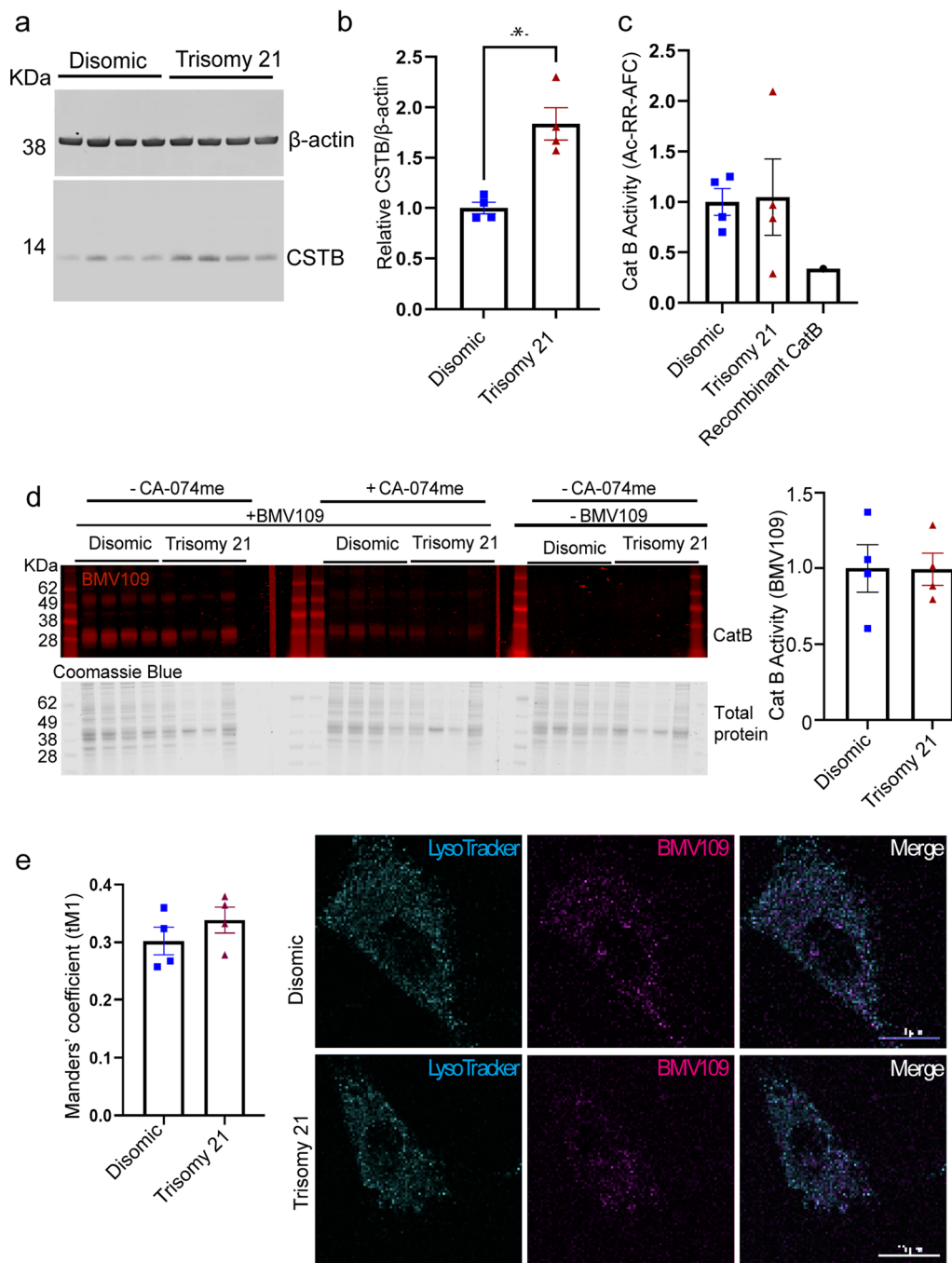


Fig. 3 Increased abundance of CSTB protein in fibroblasts isolated from individuals who have trisomy of Hsa21 is not sufficient to decrease total or lysosomal cathepsin activity compared to disomic matched cells. Cathepsin B activity and CSTB protein abundance were measured in human primary fibroblasts. **a, b** Trisomy of chromosome 21 significantly increases CSTB protein abundance as measured by western blot (Mann–Whitney U test $p=0.0286$). **c** Trisomy of chromosome 21 does not alter total cathepsin B activity as measured by biochemical assay (rate of cleavage of Ac-RR-AFC), (Mann–Whitney U test $p=0.8857$) or **d** by BMV109 fluorescence (red) quantified by in gel assay based upon enzyme identification by molecular weight (28 kDa) normalized to total protein measured by Coomassie blue (Mann–Whitney U test $p=0.6857$). **e** Trisomy of Hsa21 does not alter cathepsin activity within lysosomes as measured by lysotracker (cyan) colocalised BMV109 fluorescence (magenta) (Manders' coefficient (disomic)=0.302; (Trisomy 21)=0.339) (Mann–Whitney U test $p=0.2000$). Individual data points are group means for $n=4$ disomic and $n=4$ trisomy 21, independent cells lines (three technical replicates for western blots and 15–20 cells per lines for immunofluorescence), error bars SEM, $p < 0.05$

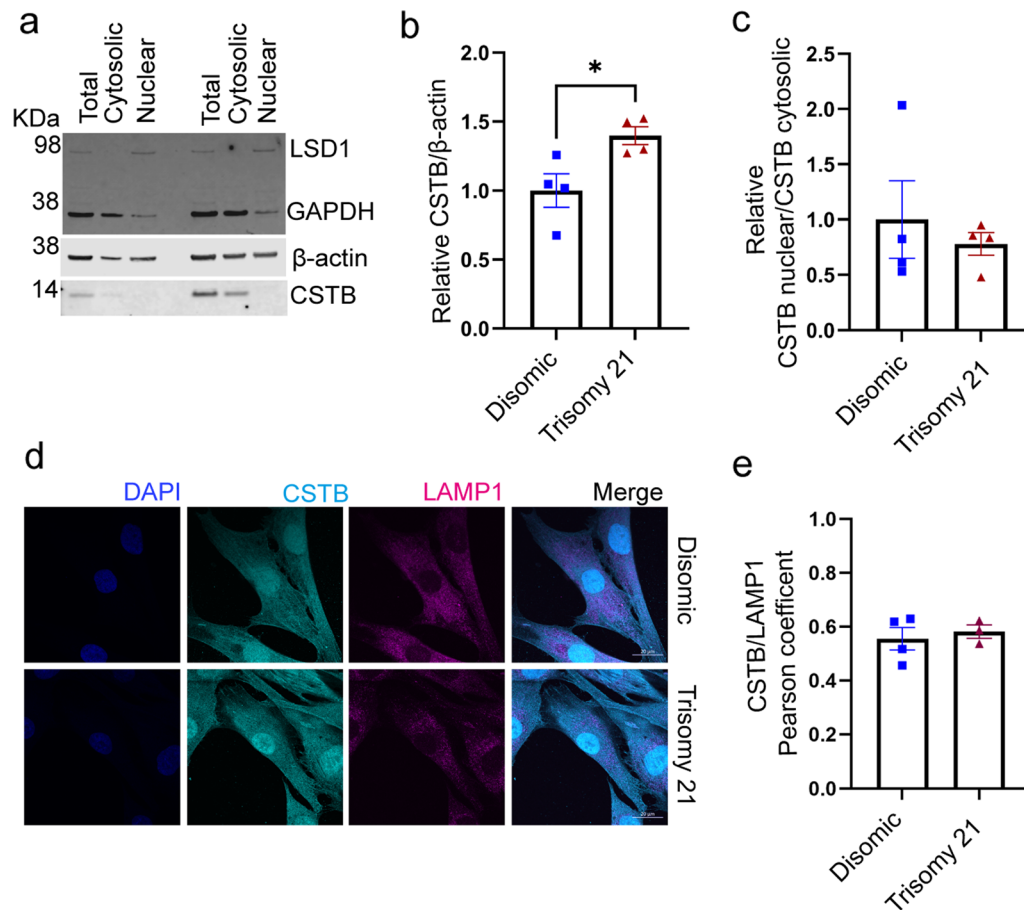


Fig. 4 Trisomy of Hsa21 does not alter the localisation of cystatin B (CSTB) to the lysosome. **a–c** Total cellular proteins from disomic and trisomy 21 human primary fibroblasts were separated into cytosolic and nuclear fraction and the abundance of CSTB quantified by western blot, LSD1 was used as a marker of the nuclear fraction. **b** Relative CSTB abundance was increased by trisomy 21 (Mann–Whitney U test $p=0.0286$) but the nuclear/cytosolic CSTB ratio was not altered (Mann–Whitney U test $p=0.8857$). **d, e** Colocalisation of CSTB (cyan) with LAMP1 (magenta) did not differ between disomic (Pearson's Correlation $R=0.555$) and trisomy 21 cells (Pearson's Correlation $R=0.582$) (Mann–Whitney U test $p=0.8571$). For **d** and **e**, individual data points are technical means of 3 technical replicates for $n=4$ disomic and $n=3$ trisomy 21, independent cell lines, error bars SEM. * $p<0.05$

on Mmu10 of the region of homology with Hsa21. This region includes *Cstb* and thus the Dp(10)2Yey model carries three copies of this gene. We undertook the study in mice from a cross of this duplicated region with a mouse model (*App*^{NL-F/NL-F}) in which the endogenous mouse *App* gene is partially humanised and carries AD causal point mutations, resulting in the accumulation of human amyloid- β within the brain of the model (Table 3) [33]. We note that we have previously studied APP processing and amyloid- β aggregation and accumulation in this cross and found that these are not significantly altered [8].

CSTB protein level was significantly increased in the cortex of 3-month old Dp(10)2Yey mice; but was not altered in littermates by the expression of human APP/amyloid- β (Fig. 6a, b). We then went on to determine if endo-peptidase activity of cathepsin B was altered at

3-months of age in the cortex of a progeny from our cross of the DS and amyloid- β accumulation models, using the same methods as for our study of human-post-mortem brain. We found no consistent effect of the Dp(10)2Yey duplication on enzyme activity, although in one experiment a modest and significant decrease in activity was observed, but this result was not replicated (Fig. 6c–f).

To determine if genes other than *CSTB* on Hsa21 when in three copies might be sufficient to modulate the activity of cathepsin B in mouse brain, we measured activity in the cortex of 3-month of age Dp1Tyb mouse model of DS, which has an additional copy of 148 Hsa21 homologous genes, including *App*, located on Mmu16 and the Dp(17)3Yey mouse model of DS, which has an additional copy of 17 Hsa21 homologues located on Mmu17. Enzyme activity was not altered by the presence of either segmental duplication, we note neither of these models

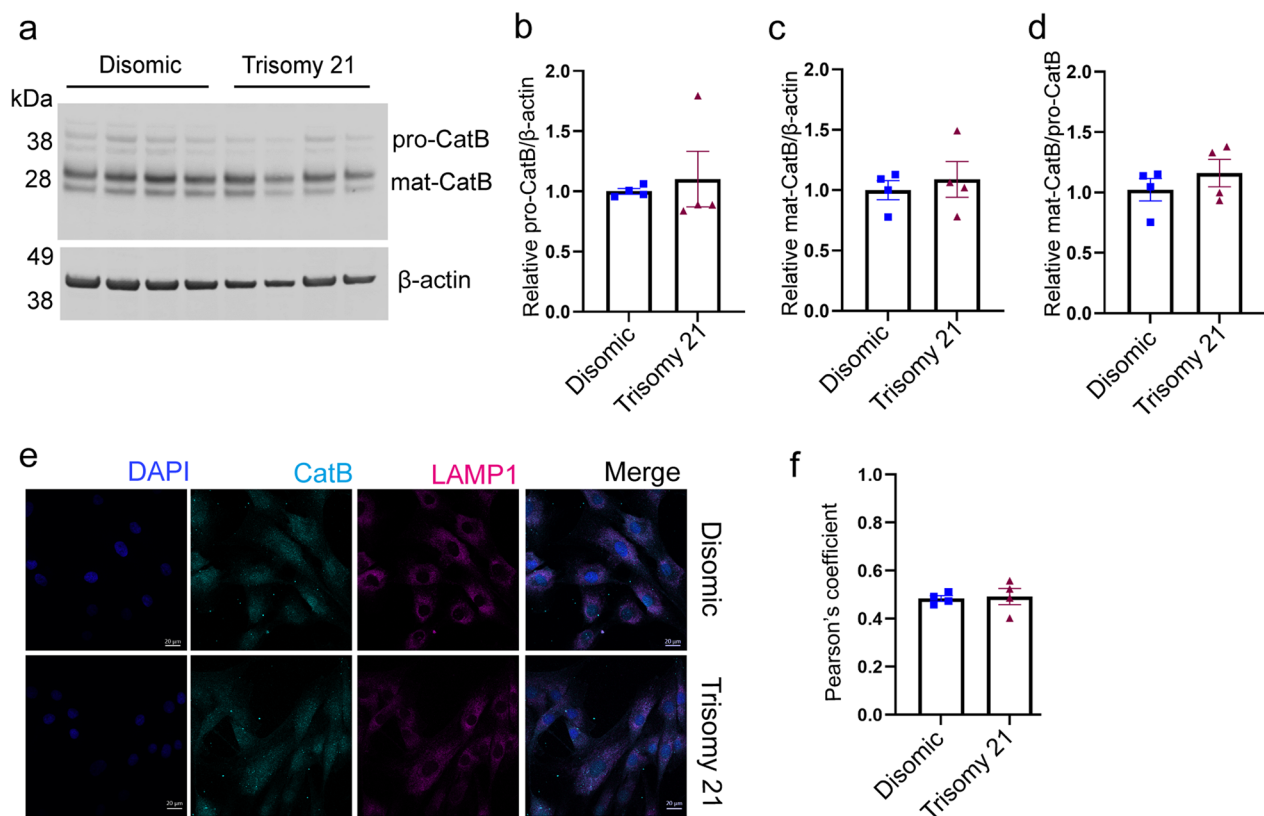


Fig. 5 Trisomy of Hsa21 does not alter cathepsin B maturation or lysosomal localisation. **a** Western blot showing pro-cathepsin B (pro-CatB) and mature cathepsin B (mat-CatB) protein levels in disomic and trisomy 21 human primary fibroblasts **b** pro-cathepsin B protein levels (Mann–Whitney U test $p=0.3429$), **c** mature cathepsin B protein level (Mann–Whitney U test $p=0.8857$), **d** mature cathepsin B/pro-cathepsin B ratio (Mann–Whitney U test $p=0.6857$) were not altered by trisomy 21. **e, f** Colocalisation of cathepsin B (cyan) with LAMP1 (magenta) was measured using immunofluorescence and no difference between disomic (Pearson's Correlation $R=0.484$) and trisomy 21 (Pearson's Correlation $R=0.493$) fibroblasts was observed (Mann–Whitney U test $p=0.6857$). Individual data points are means of 3 technical replicates for $n=4$ disomic and $n=4$ trisomy 21 independent cell lines, error bars SEM

carries an additional copy of *Cstb*. These data indicate that three copies of *Cstb* is not sufficient to modulate cathepsin B activity in a mouse model of AD-DS, consistent with our previous findings from a segmental duplication model of *Cstb* [34], nor is an additional copy of Hsa21 homologues encoded on Mmu16 or Mmu17 sufficient to alter activity.

Discussion

Our data demonstrate that three copies of Hsa21 raises the abundance of CSTB protein in the brains of individuals who have AD-DS, in the Dp2(10)Yey mouse model of DS, and in fibroblasts isolated from children who have DS compared with matched disomic controls, consistent with our primary hypothesis. Increased abundance of this endogenous inhibitor of cysteine cathepsins could modulate key aspects of neurobiology by the inhibition of the activity of cathepsin B. This may be particularly relevant in AD pathogenesis in which abundance and activity of the enzyme is upregulated and has been suggested to

impact on a number of key disease mechanisms, including APP processing, amyloid- β catabolism, and the neuroinflammatory response to pathology; particularly via the activation of inflammasomes [35–37].

Here, we demonstrate that the number of cathepsin B⁺ cells, and the activity of cathepsin B is significantly increased in people who have EOAD compared with those undergoing healthy ageing, supporting the proposed role of the enzyme as a potential therapeutic target in AD. This is consistent with reports of elevated cathepsin B associated with amyloid plaques in LOAD [38, 39] and raised cathepsin B in plasma of individuals with AD [40, 41]. We note that decreased cathepsin B abundance has been reported to occur in monocytes of individuals with AD [41, 42], indicating that ubiquitous increase in the enzyme may not occur in all cell types.

Although the number of cathepsin B⁺ cells is similarly increased in individuals who have AD-DS, we find that the activity of the enzyme is significantly lower than in matched individuals who have EOAD consistent with our

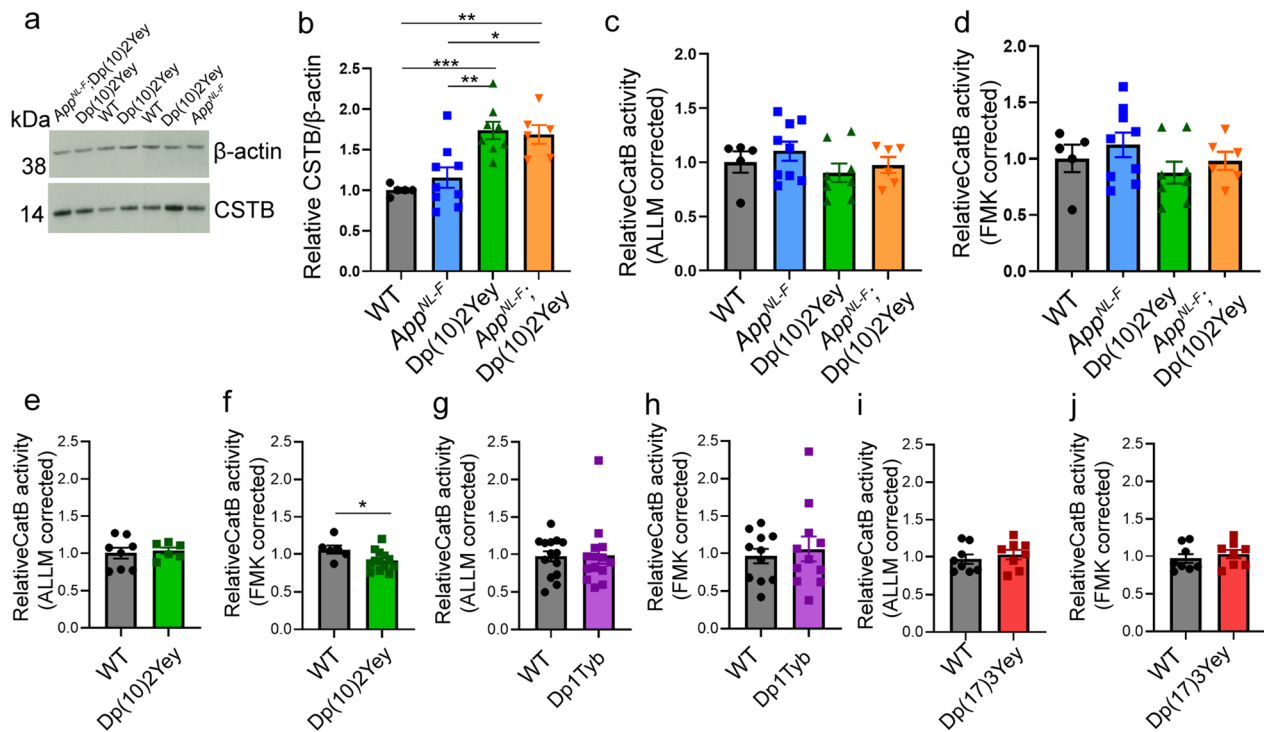


Fig. 6 Three copies of *Cstb* increase cystatin B (CSTB) in the cortex of mouse models of AD-DS but do not alter cathepsin B activity. **a, b** CSTB protein abundance (determined by western blot) was measured in cortex of a 3-month old mouse model of AD-DS (progeny from a cross of *Dp(10)2Yey* and *App^{NL-F/NL-F}*), including in *Dp(10)2Yey* and *Dp(10)2Yey; App^{NL-F/NL-F}* genotypes which have three copies of *Cstb*. The abundance of CSTB was significantly increased by the *Dp(10)2Yey* region (ANOVA $F(1,22) = 31.269$, $p < 0.0001$). Significantly higher CSTB levels were detected in *Dp(10)2Yey* compared to wildtype (WT) (pairwise comparisons with Bonferroni correction, $p < 0.001$) and *App^{NL-F/NL-F}* (pairwise comparisons with Bonferroni correction, $p = 0.003$) cortex. Significantly higher CSTB levels were detected in *Dp(10)2Yey; App^{NL-F/NL-F}* cortex compared to wildtype (WT) (pairwise comparisons with Bonferroni correction, $p = 0.005$) and *App^{NL-F/NL-F}* (pairwise comparisons with Bonferroni correction, $p = 0.015$) cortex. **c-h** Cathepsin B activity determined by biochemical assay (rate of cleavage of Ac-RR-AFC, corrected for non-specific activity measured in samples inhibited by **c, e, g, i** ALLM or **d, f, h, j** FMK(z-FA-FMK). **c, d** No difference in cathepsin B activity was detected in cortex of 3-month old mice carrying the *Dp(10)2Yey* segmental duplication compared to animals without the duplication including WT and *App^{NL-F/NL-F}* genotypes (progeny from a cross of *Dp(10)2Yey* and *App^{NL-F/NL-F}* mice); **c** ALLM (ANOVA $F(1,22) = 1.325$, $p = 0.262$) or **d** FMK (ANOVA $F(1,22) = 1.142$ or $p = 0.297$). No difference in cathepsin B activity was detected in cortex from 3-month-old mice homozygous for the *App^{NL-F}* allele that results in amyloid- β accumulation (*App^{NL-F/NL-F}* and *Dp(10)2Yey; App^{NL-F/NL-F}* genotypes); **c** ALLM (ANOVA $F(1,22) = 0.571$, $p = 0.458$) or **d** FMK (ANOVA $F(1,22) = 0.815$ or $p = 0.376$). **e** No difference in cathepsin B activity was detected in cortex of 3-month old mice with the *Dp(10)2Yey* segmental duplication (generated from a cross to C57BL/6J) ALLM (ANOVA $F(1,10) = p = 0.118$). **f** A modest reduction in cathepsin B activity was detected in cortex of 3-month old mice with the *Dp(10)2Yey* segmental duplication (generated from a cross to C57BL/6J) FMK (ANOVA $F(1,15) = 5.542$, $p = 0.033$). No difference in cathepsin B activity was detected in cortex of 3-month-old mice with the *Dp11Yb* segmental duplication (generated from a cross to C57BL/6J), **g** ALLM (ANOVA $F(1,24) = 0.010$, $p = 0.923$) or **h** FMK (ANOVA $F(1,18) = 0.013$ or $p = 0.909$). **i, j** No difference in cathepsin B activity was detected in cortex of 3-month old mice with the *Dp(17)3Yey* segmental duplication (generated from a cross to C57BL/6J), **i** ALLM (ANOVA $F(1,12) = 0.543$, $p = 0.475$) or **j** FMK (ANOVA $F(1,12) = 0.731$ or $p = 0.409$). Individual data points are technical means for independent biological samples, error bars SEM. * $p < 0.05$, ** $p < 0.01$, *** $p < 0.001$. Male and female mice were used and sex was included as a variable in the ANOVA, cohort details Table 3

hypothesis; this indicates that trisomy of Hsa21 impairs enzyme activity during end-stage disease. These changes occur independently of neurofibrillary tangle stage, or the colocalisation of the enzyme with IBA1⁺ microglia and may result from the additional copy of *CSTB* carried by individuals who have DS.

We observe no difference in the activity of cathepsin B between individuals who have AD-DS and euploid individuals who do not have AD and are ageing

healthily, in contrast to the upregulation in activity we observed in disomic individuals who had EOAD. The majority of individuals who have DS develop early onset-AD in mid-life [43], thus we could not source adult post-mortem brain tissue from individuals who had DS but who did not have AD, to determine if the level of cathepsin activity in absence of AD neuropathology differs between people with DS with and disomic individuals in the brain.

To investigate the role of increased CSTB further, we used mouse and human cellular preclinical models, that have an additional copy of *CSTB* which encodes cystatin B. In these model systems we observed that the abundance of CSTB protein is increased but that cathepsin B enzyme activity is not robustly altered. We also observed this in the cortex of a DS-AD mouse model (*App*^{NL-F/NL-F}; Dp(10)2Yey) at 3-months of age, which expresses human amyloid- β but has yet to accumulate significant aggregated peptide [8, 33]. Previous studies using aged transgenic *APP* mouse models have indicated an increase in cathepsin B protein abundance [44]. However, consistent with our results enhanced cathepsin B activity was also not observed in another amyloid- β accumulation model at 6-months of age [31]. In this study by Yang and colleagues, loss of a copy of *Cstb* was sufficient to increase cathepsin B activity in the mouse brain, but here we find conversely that an additional copy of *Cstb* is not sufficient to decrease cathepsin B activity. This is consistent with our previous report that duplication of the *Cstb* gene is also not sufficient to alter cathepsin B activity in the cortex of a mouse model, and underlies that loss and gain of function of a gene do not always have inverse consequences [34].

A previous study has reported a small but significant increase in cathepsin B activity in fibroblasts isolated from infants and children who had DS and typically developing controls [23]. We note that two of our trisomy 21 fibroblast lines (AG07438 and AG05397) and all of our disomic control lines differ from the lines studied by Jiang and colleagues, thus biological variation between the cell line used may contribute to the differences in our results. We note that our cellular preclinical model will not recapitulate cell-type specific functions of CSTB, such as its role at the synapse in neurons [45] or proposed regulatory role in microglia [46].

Our data indicate that the raised abundance of CSTB protein is not sufficient to modulate cathepsin B activity in a range of model systems, perhaps because of the homeostatic regulation of the interaction of enzyme and inhibitor. However, our preclinical models do not recapitulate all aspects of end-stage (Braak VI) AD, notably the development of tau neurofibrillary pathology, a neuroinflammatory reaction to neuropathology and changes to the blood brain barrier, all of which may contribute to the dramatic increase in cathepsin B activity we observed in individuals who have EOAD. Thus, further research is required to determine if raised CSTB may contribute to altered AD-associated cathepsin B activity in the context of these key aspects of the disease. This is important, as the changed AD-associated cathepsin B activity we observe, could contribute to differences in the progression of AD in people who have DS.

Moreover, understanding why the activity is different in the presence of an additional copy of Hsa21 could provide significant novel insight into the underlying biology. Furthermore, our data indicate that targeting cathepsin B activity in people who have DS (i.e., an additional copy of Hsa21) is unlikely to have the same therapeutic effect as in individuals who have AD in the general population and that alternative targets should be considered for this important group of individuals who have a greatly elevated risk of early-onset disease.

Here we find that cathepsin D activity is not significantly altered in the brains of individuals who have AD-DS compared to disomic healthy ageing controls; although our study may be underpowered. A previous study had shown that cathepsin D activity is robustly decreased in fibroblasts isolated from individuals who have DS compared to disomic controls [23]. Moreover, in a study of human post-mortem brain by Curtis and colleagues, cathepsin D activity was observed to be decreased in older adults who had DS (40–65 years of age), [47]. They found that activity was not altered in younger adults who had DS (15–40 years of age) or in the brains of older adults (77–91 years of age) from the general population who had Late-onset AD (LOAD). Another report suggests a modest increase in cathepsin D activity occurs in younger individuals who have DS (2–45 years of age) [48], further studies are required to investigate these differences. Additionally, the number of cathepsin D positive cells, the abundance of cathepsin D transcript and protein is increased in LOAD, including associated with plaques [38, 49–51]. Further research is required to understand how cathepsin D abundance and cellular location affects its function over the course of disease.

Our data indicate that disomic individuals who have EOAD have decreased cathepsin D activity, this suggests that decreased enzyme activity may be attributable to the early development of AD in mid-life rather than a direct effect of three copies of Hsa21 and these processes may differ in EOAD and LOAD. This could relate to the elevated abundance of amyloid- β or APP-C-terminal fragment, which have been proposed to inhibit cathepsin D activity [23, 52] and also underlies the early development of AD-DS [3]. Additional studies to quantify enzyme activity across disease development, in independent cases, and correlate this with amyloid- β or APP-C-terminal fragment abundance are needed to verify this hypothesis.

Study limitations

Here we study a case series of individuals who had EOAD and did, or did not, have DS, compared with healthily ageing individuals from the general population. As

outlined, the demographics of the groups differed. In particular, the healthy ageing group was older than the AD-DS and EOAD groups, and the Braak tangle stage of the AD-DS and EOAD groups were not perfectly matched. To address these limitations, we included age at death as a covariant in our analysis and performed a sub-analysis of our Braak VI stage cases. In addition, here we only studied 10 individuals of each case-type and thus intra-individual variability may confound our results, and confirmation of our key findings in independent cases would be beneficial. It was not possible to study aged-matched cases of human-post-mortem material from individuals who have DS but did not have AD, because of the early development of AD neuropathology in people who have DS [43]. Thus, we could not determine if changed cathepsin activity occurs in the brain prior to the development of AD in people who have DS. Similarly, the increased number of IBA1⁺ and CatB⁺ cells we observed in people who have AD-DS compared with disomic individuals who were ageing healthily may have a neurodevelopmental cause and not be the direct result of AD.

Here we tested our hypothesis that raised CSTB protein leads to reduced cathepsin B activity, as suggested by our human post-mortem analysis, in both human cellular and mouse models using a range of technical approaches. As outlined above, both preclinical systems have limitations and do not model all aspects of the biology of the human brain.

Conclusion

Our data indicate both similarities and differences between EOAD in people who have and do not have DS. We find that cathepsin B activity is lower in people with DS when they develop AD compared with disomic individuals. In contrast, EOAD is associated with a similar decrease in cathepsin D activity in people with and without an additional copy of Hsa21. We also find that the number of cathepsin B⁺ cells and the abundance of cathepsin B protein does not differ between AD-DS and EOAD cases. However, the abundance of CSTB is significantly higher in the temporal cortex of cases of AD-DS compared with EOAD or healthy ageing. We also find that in both a human cellular and mouse model of DS, CSTB protein levels are increased but this is not sufficient to change cathepsin B activity. Research to understand these similarities and differences will both ensure that individuals who have DS have access to the most appropriate AD therapeutics and provides unique insight into the biology of AD pathogenesis by understanding how an additional copy of genes on Hsa21 can modulate disease.

Abbreviations

AD	Alzheimer's disease
AD-DS	Alzheimer's disease in individuals who had Down syndrome
AFC	Amino-4-trifluoromethyl coumarin
ALLM	N-Acetyl-L-leucyl-L-leucyl-L-methioninal
APP	Amyloid precursor protein
CatB	Cathepsin B
CatD	Cathepsin D
CSTB	Cystatin B
DMEM	Dulbecco's modified eagle medium
DS	Down syndrome
EDTA	Ethylenediaminetetraacetic acid
EOAD	Early-onset Alzheimer's disease
EPM1	Unverricht-Lundborg type
LDS	Lithium dodecyl sulphate
MCA	7-Methoxycoumarin-4-acetic acid
PFA	Paraformaldehyde
PMI	Post-mortem interval
SEM	Standard error of the mean
WT	Wildtype

Supplementary Information

The online version contains supplementary material available at <https://doi.org/10.1186/s40478-023-01632-8>.

Additional file 1. Supplementary Figure 1: changes to cathepsin B and cathepsin D activity in a sub analysis of EOAD and AD-DS Braak VI cases.

Acknowledgements

The authors thank Eugene Yu (Rosewell Cancer Research Institute, USA) for Dp(10)2Yey and Dp(17)3Yey mouse models and Takaomi Saido (Riken Institute, Japan) for the *App*^{NL-F/NL-F} mouse model. We thank the Coriell Cell repositories, USA for the human fibroblast cell lines used in this study. We would like to thank the South West Dementia Brain Bank (SWDBB), and the generosity of the donors and their families for providing brain tissue for this study. We would also like to thank Connor Scott (UCL) for offering valuable guidance regarding the process of immunostaining. We thank Oke Avwenagha (UCL) for her assistance with this project. For the purpose of Open Access, the authors have applied a CC BY public copyright licence to any Author Accepted Manuscript version arising from this submission.

Author contributions

EMCF, and FKW designed the research and applied for ethical permission for research; YW, AM, DL, PM, SN, KC, and FKW performed research; YW, KC, PM, and FKW analysed data; YW, PM, DL, SN, KC, FD, MV, AM, EMCF, and FKW edited the paper; FKW wrote the paper; FD and MV contributed reagents/analytic tools and procedures.

Funding

Y.W. is funded by an Alzheimer's Research UK Senior Research Fellowship held by F.K.W. (ARUK-SRF2018-001). <https://www.alzheimersresearchuk.org/research> F.K.W. is also supported by the UK Dementia Research Institute (UKDRI-1014) which receives its funding from DRI Ltd, funded by the UK Medical Research Council, Alzheimer's Society and Alzheimer's Research UK. <https://ukdri.ac.uk/> <https://mrc.ukri.org/> <https://www.alzheimersresearchuk.org/research> <https://www.alzheimers.org.uk/> F.K.W. also received funding that contributed to the work in this paper from the Rosetrees Trust MB2020\100003. <https://rosetreestrust.co.uk/> E.M.C.F. received funding from a Wellcome Trust Strategic Award (grant number: 098330/Z/12/Z) awarded to The London Down Syndrome (LonDownS) Consortium (E.M.C.F) and a Wellcome Trust Joint Senior Investigators Award (grant numbers: 098328, 098327). <https://wellcome.org/> M.V. was the recipient of ERC Starting Grant CHEMCHECK (679921) and a Gravity Program Institute for Chemical Immunology tenure track grant by NWO. The funders had no role in study design, data collection and analysis, decision to publish, or preparation of the manuscript. We would like to thank the South West Dementia Brain Bank (SWDBB), their donors and donor's families for providing brain tissue for this study. Tissue for this study was provided with support from the Brains for Dementia Research

(BDR) programme, jointly funded by Alzheimer's Society UK and Alzheimer's Society. The SWDBB is further supported by BRACE (Bristol Research into Alzheimer's and Care of the Elderly).

Availability of data and materials

The datasets generated during the current study available from the corresponding author on reasonable request.

Declarations

Ethics approval and consent to participate

Human tissue The procurement and use of human tissues in this study was in accordance with the UK Human Tissue Act 2004. The study was reviewed and approved by NHS Research Ethics committee, London-Queen Square (REC 09/H0716/57). All samples were supplied, anonymized by the South West Dementia Brain Bank, Bristol University, UK, and had full research consent (REC 18/SW/0029). **Animal research** All experiments were undertaken in accordance with the Animals (Scientific Procedures) Act 1986 (United Kingdom), after local institutional ethical review by the Medical Research Council, University College London under licence from the UK government and reported in accordance with ARRIVE 2.0 guidelines.

Consent to publication

Not applicable.

Competing interests

The authors declare that they have no competing interests.

Author details

¹The UK Dementia Research Institute, University College London, Queen Square, London WC1N 3BG, UK. ²Department of Neuromuscular Diseases, Queen Square Institute of Neurology, University College London, Queen Square, London WC1N 3BG, UK. ³Department of Medical BioSciences, Radboudumc, Geert Grooteplein Zuid 28, 6525 GA Nijmegen, The Netherlands. ⁴Institute for Chemical Immunology, Geert Grooteplein Zuid 28, 6525 GA Nijmegen, The Netherlands.

Received: 20 June 2023 Accepted: 4 August 2023

Published online: 14 August 2023

References

- Fortea J et al (2021) Alzheimer's disease associated with Down syndrome: a genetic form of dementia. *Lancet Neurol* 20(11):930–942
- Rovelet-Lecrux A et al (2006) APP locus duplication causes autosomal dominant early-onset Alzheimer disease with cerebral amyloid angiopathy. *Nat Genet* 38(1):24–26
- Sawa M et al (2022) Impact of increased APP gene dose in Down syndrome and the Dp16 mouse model. *Alzheimers Dement* 18(6):1203–1234
- Doran E et al (2017) Down syndrome, partial trisomy 21, and absence of Alzheimer's disease: the role of APP. *J Alzheimers Dis* 56(2):459–470
- Prasher VP et al (1998) Molecular mapping of Alzheimer-type dementia in Down's syndrome. *Ann Neurol* 43(3):380–383
- Alic I et al (2021) Patient-specific Alzheimer-like pathology in trisomy 21 cerebral organoids reveals BACE2 as a gene dose-sensitive AD suppressor in human brain. *Mol Psychiatry* 26:5766–5788
- Garcia-Cerro S et al (2017) Normalizing the gene dosage of Dyrk1A in a mouse model of Down syndrome rescues several Alzheimer's disease phenotypes. *Neurobiol Dis* 106:76–88
- Mumford P et al (2022) Genetic mapping of APP and amyloid-beta biology modulation by trisomy 21. *J Neurosci* 42(33):6453–6468
- Tosh JL et al (2021) Genetic dissection of down syndrome-associated alterations in APP/amyloid-beta biology using mouse models. *Sci Rep* 11(1):5736
- Wiseman FK et al (2018) Trisomy of human chromosome 21 enhances amyloid-beta deposition independently of an extra copy of APP. *Brain* 141(8):2457–2474
- Zheng Q et al (2022) USP25 inhibition ameliorates Alzheimer's pathology through the regulation of APP processing and Abeta generation. *J Clin Invest* 132(5):e152170
- Flores-Aguilar L et al (2020) Evolution of neuroinflammation across the lifespan of individuals with Down syndrome. *Brain* 143(12):3653–3671
- Martini AC et al (2020) Distribution of microglial phenotypes as a function of age and Alzheimer's disease neuropathology in the brains of people with Down syndrome. *Alzheimers Dement (Amst)* 12(1):e12113
- Palmer CR et al (2021) Altered cell and RNA isoform diversity in aging Down syndrome brains. *Proc Natl Acad Sci USA* 118(47):e2114326118
- Wilcock DM et al (2015) Down syndrome individuals with Alzheimer's disease have a distinct neuroinflammatory phenotype compared to sporadic Alzheimer's disease. *Neurobiol Aging* 36(9):2468–2474
- Zheng Q et al (2021) Trisomy 21-induced dysregulation of microglial homeostasis in Alzheimer's brains is mediated by USP25. *Sci Adv* 7(1):eabe1340.
- Bellenguez C et al (2022) New insights into the genetic etiology of Alzheimer's disease and related dementias. *Nat Genet* 54(4):412–436
- Stoka V, Turk V, Turk B (2016) Lysosomal cathepsins and their regulation in aging and neurodegeneration. *Ageing Res Rev* 32:22–37
- Hook G, Kindy M, Hook V (2023) Cathepsin B deficiency improves memory deficits and reduces amyloid- β in hA β PP mouse models representing the major sporadic Alzheimer's disease condition. *J Alzheimers Dis* 93(1):33–46
- Sun B et al (2008) Cystatin C-cathepsin B axis regulates amyloid beta levels and associated neuronal deficits in an animal model of Alzheimer's disease. *Neuron* 60(2):247–257
- Hook V et al (2020) Cathepsin B in neurodegeneration of Alzheimer's disease, traumatic brain injury, and related brain disorders. *Biochim Biophys Acta Proteins Proteom* 1868(8):140428
- Heneka MT (2017) Inflammasome activation and innate immunity in Alzheimer's disease. *Brain Pathol* 27(2):220–222
- Jiang Y et al (2019) Lysosomal dysfunction in down syndrome is APP-dependent and mediated by APP- β CTF (C99). *J Neurosci* 39(27):5255–5268
- Suire CN, Leissring MA (2021) Cathepsin D: a candidate link between amyloid β -protein and tauopathy in Alzheimer disease. *J Exp Neurol* 2(1):10–15
- Edgington-Mitchell LE et al (2016) Legumain is activated in macrophages during pancreatitis. *Am J Physiol-Gastrointest Liver Physiol* 311(3):G548–G560
- Dunn KW, Kamocka MM, McDonald JH (2011) A practical guide to evaluating colocalization in biological microscopy. *Am J Physiol Cell Physiol* 300(4):C723–C742
- Braak H et al (2006) Staging of Alzheimer disease-associated neurofibrillary pathology using paraffin sections and immunocytochemistry. *Acta Neuropathol* 112(4):389–404
- Nakanishi H et al (1994) Age-related changes in activities and localizations of cathepsins D, E, B, and L in the rat brain tissues. *Exp Neurol* 126(1):119–128
- Pinto B et al (2020) Rescuing over-activated microglia restores cognitive performance in juvenile animals of the Dp(16) mouse model of down syndrome. *Neuron* 108(5):887–904.e12
- Verdoes M et al (2013) Improved quenched fluorescent probe for imaging of cysteine cathepsin activity. *J Am Chem Soc* 135(39):14726–14730
- Yang DS et al (2011) Reversal of autophagy dysfunction in the TgCRND8 mouse model of Alzheimer's disease ameliorates amyloid pathologies and memory deficits. *Brain* 134(Pt 1):258–277
- Alakurtti K et al (2005) Loss of lysosomal association of cystatin B proteins representing progressive myoclonus epilepsy, EPM1, mutations. *Eur J Hum Genet* 13(2):208–215
- Saito T et al (2014) Single App knock-in mouse models of Alzheimer's disease. *Nat Neurosci* 17(5):661–663
- Wu Y et al (2021) The effects of Cstb duplication on APP/amyloid-beta pathology and cathepsin B activity in a mouse model. *PLoS ONE* 16(7):e0242236
- Chevriaux A et al (2020) Cathepsin B is required for NLRP3 inflammatory activation in macrophages, through NLRP3 interaction. *Front Cell Dev Biol* 8:167

36. Embury CM et al (2017) Cathepsin B improves β -amyloidosis and learning and memory in models of Alzheimer's disease. *J Neuroimmune Pharmacol* 12(2):340–352
37. Oberstein TJ et al (2020) The role of cathepsin B in the degradation of A β and in the production of A β peptides starting with Ala2 in cultured astrocytes. *Front Mol Neurosci* 13:615740
38. Cataldo AM, Nixon RA (1990) Enzymatically active lysosomal proteases are associated with amyloid deposits in Alzheimer brain. *Proc Natl Acad Sci USA* 87(10):3861–3865
39. Cataldo AM et al (1991) Lysosomal hydrolases of different classes are abnormally distributed in brains of patients with Alzheimer disease. *Proc Natl Acad Sci USA* 88(24):10998–11002
40. Sundelöf J et al (2010) Higher cathepsin B levels in plasma in Alzheimer's disease compared to healthy controls. *J Alzheimers Dis* 22(4):1223–1230
41. Morena F et al (2017) A comparison of lysosomal enzymes expression levels in peripheral blood of mild- and severe-Alzheimer's disease and MCI patients: implications for regenerative medicine approaches. *Int J Mol Sci* 18(8):1806
42. Tiribuzi R et al (2014) miR128 up-regulation correlates with impaired amyloid β (1–42) degradation in monocytes from patients with sporadic Alzheimer's disease. *Neurobiol Aging* 35(2):345–356
43. Fortea J et al (2020) Clinical and biomarker changes of Alzheimer's disease in adults with Down syndrome: a cross-sectional study. *Lancet* 395(10242):1988–1997
44. Sun Y et al (2015) Translational study of Alzheimer's disease (AD) biomarkers from brain tissues in A β PP/PS1 mice and serum of AD patients. *J Alzheimers Dis* 45(1):269–282
45. Penna E et al (2019) Cystatin B involvement in synapse physiology of rodent brains and human cerebral organoids. *Front Mol Neurosci* 12:195
46. Kopitar-Jerala N (2015) The role of Stefin B in neuro-inflammation. *Front Cell Neurosci* 9:458
47. Curtis ME, Yu D, Pratico D (2020) Dysregulation of the retromer complex system in down syndrome. *Ann Neurol* 88(1):137–147
48. Di Domenico F et al (2013) Impairment of proteostasis network in Down syndrome prior to the development of Alzheimer's disease neuropathology: redox proteomics analysis of human brain. *Biochim Biophys Acta* 1832(8):1249–1259
49. Chai YL et al (2019) Lysosomal cathepsin D is upregulated in Alzheimer's disease neocortex and may be a marker for neurofibrillary degeneration. *Brain Pathol* 29(1):63–74
50. Bordi M et al (2016) Autophagy flux in CA1 neurons of Alzheimer hippocampus: Increased induction overburdens failing lysosomes to propel neuritic dystrophy. *Autophagy* 12(12):2467–2483
51. Cataldo AM et al (1995) Gene expression and cellular content of cathepsin D in Alzheimer's disease brain: evidence for early up-regulation of the endosomal-lysosomal system. *Neuron* 14(3):671–680
52. Suire CN et al (2020) Cathepsin D regulates cerebral A β 42/40 ratios via differential degradation of A β 42 and A β 40. *Alzheimers Res Ther* 12(1):80

Publisher's Note

Springer Nature remains neutral with regard to jurisdictional claims in published maps and institutional affiliations.

Ready to submit your research? Choose BMC and benefit from:

- fast, convenient online submission
- thorough peer review by experienced researchers in your field
- rapid publication on acceptance
- support for research data, including large and complex data types
- gold Open Access which fosters wider collaboration and increased citations
- maximum visibility for your research: over 100M website views per year

At BMC, research is always in progress.

Learn more biomedcentral.com/submissions

